NTNU – Trondheim
Norwegian University of
Science and Technology

Theoretical study of Osmotic and Swelling Pressures with Experimental Investigation of Threshold Capillary Pressure in Shales

Aftab Hussain Arain

Petroleum Engineering
Submission date: July 2015
Supervisor: Andreas Bauer, IPT

Norwegian University of Science and Technology
Department of Petroleum Engineering and Applied Geophysics

Acknowledgment

Foremost, I must thank Almighty ALLAH for bestowing upon me his blessing and giving me the strength for making this attempt a fruitful one.

I would like to express my profound gratitude to my supervisor, Andreas Bauer for his exceptional supervision, valuable research guidance and continuous support at every stage of this thesis.

I would like to thanks Muhammad Hossain Bhuiyan, Researcher, SINTEF, for his support, suggestion and help during capillary threshold pressure experiments.

I want to extend my gratitude to NED University of Engineering and Technology, Karachi, Pakistan, for providing me financial support to pursue a master degree at Norwegian University of Science and Technology (NTNU).

I would also like to thank Norwegian University of Science and Technology (NTNU) for giving me an opportunity to study in this prestigious institute.

Finally, my deepest gratitude for my Parents for their endless love, support & encouragement and who have been the pillars of my success in all that I have achieved so far.

Abstract

Shales are considered to be the most problematic and challenging formation encounter during drilling. The major problems encountered during shale drilling are related to wellbore instability. The unfavorable interaction between the shale and the water-base mud is considered to be the primary cause of shale instability. The fluid invasion increases the pore pressure and reduces the shale strength by altering the stress state of shale. Whereas, hydration of shale can cause the development of swelling stress and results in wellbore instability.

The initial plan for this thesis was to conduct laboratory experiments to measure the osmotic and swelling pressures in shales as a function of stress. Therefore, the major part of this thesis comprises theoretical knowledge of osmotic and swelling pressure. Unfortunately the only available equipment was engaged for SINTEF's own project work, which was threshold capillary pressure measurement on shale. Therefore, in the later stage in terms of time, it was decided to include the laboratory experiments of capillary threshold pressure in shale.

The shales having wellbore instability problems can be drilled with oil-base mud. The low permeable water-wet shales generate high capillary forces which prevents the fluid flow into the shale even at significant overbalance pressures. However, if the wellbore pressure would be adequately high enough, it may overcome the capillary forces and invade the formation and cause wellbore instability. Therefore, during process it must be known that how much the wellbore pressure should be to avoid invasion in shale.

The capillary threshold pressure was measured for two different types of shale sample by using base oil as non-wetting phase. The approach used for the measurement was standard approach, which includes consolidation phase and capillary threshold pressure phase. The experiments were performs on two different shale samples; one was Pierre shale and another was Field shale. In first test only threshold capillary pressure was measured, while in second test the capillary breakthrough pressure was measured in addition to the capillary threshold pressure. The estimated capillary threshold pressure for Pierre shale was 0.5 MPa and for Field shale was 0.3 MPa. Also the estimated capillary breakthrough pressure for Filed shale was 0.5 MPa.

Table of Contents

List of Figures

List of Tables

List of Symbols

σ	Interfacial tension between wetting and non-wetting
σ^{eff}	Effective stress
σ_r^{eff}	Effective radial stress
σ_θ^{eff}	Effective tangential stress
σ_h	Minimum horizontal stress
η_f	Viscosity of pore fluid
μ	Viscosity of drilling fluid
α_m	Membrane efficiency
τ_D	Diffusion time
$\emptyset$	Porosity
θ	Contact angle
$\Delta\Pi$	Osmotic pressure difference
A	Cross-sectional area of shale
$a_{w,shale}$	Water activity of shale
$a_{w,mud}$	Water activity of drilling mud
C_D	Pore pressure diffusion coefficient
C_{mud}	Concentration of ions in mud
C_{shale}	Concentration of ions in shale
D	Diffusion coefficient
G_{fr}	Shear modulus of the rock frame
J	Diffusion flux
K_f	Bulk modulus of fluid
K_{fr}	Drained bulk modulus
k	Permeability
L	Length of shale
l_D	Diffusion length
P	Vapor pressure of shale
P_c	Capillary threshold pressure
P_{mud}	Hydrostatic pressure of drilling mud
P_{nw}	Pressure of non-wetting phase
P_{shale}	Pore pressure of shale
P_w	Pressure of wetting phase

P_{water}	Vapor pressure of pure water
P_{well}	Wellbore pressure
ΔP	Pressure difference
R	Gas constant
r	Pore throat radius
T	Absolute temperature
T_o	Tensile strength
q	Total flow
$\bar{V}_w$	Molar volume of water
v_s	Mobility of solute (ions)
v_w	Mobility of water
Δx	Length of shale

Chapter 01
Introduction

1.1. Background

Wellbore instability is one of the most serious technical problems in the oil industry [1-4]. Shales are considered to be the main cause of wellbore instability [5, 6]. Shales make up to 75% of drilled formation and over 90% of the wellbore instability problems are related to the drilling through shales [7-9].

Wellbore instability can lead to lost in drilling time, increases in drilling cost, and abandonment of the well [1]. It is estimated that this problem costs the oil industry more than $500 million/year [1, 2, 6].

There are many factors which are considered to be responsible for instability in shale. The primary cause of wellbore instability is the unfavorable interaction between the shale and the water-base mud [5, 6]. These interactions are complex and include mechanical, chemical, physical and hydraulic phenomena [6]. The overall effect of these interactions is mainly related to the flow of water molecules and ions into or out of shale[8].

The invasion of water molecules and ions raise the pore pressure of shale, which alter the effective stress around the wellbore. In addition to this, hydration of clay minerals in shale develop the swelling stress, which ultimately results in wellbore instability of shale [4]. The physico-chemical and mechanical properties of shale around the wellbore can be greatly effect by such problems [8].

1.2. Problem Formulation

Shales are relatively weak rocks and contain significant amounts of clay minerals. The mud filtrate invades the shale, when shale comes in contact with water-base mud. This mud invasion increase the pore pressure and cause swelling of shale, and ultimately results in wellbore failure [4]. While drilling through shale with water-base mud, several different interactions can occur between the drilling fluid and the shale [10].

The first interaction is the hydraulic flow which is based on Darcy's law. In hydraulic flow, the fluid flow occurs due to pressure gradient between wellbore pressure and shale pore pressure.

In overbalance drilling, the flow will be from wellbore into shale. While in underbalance drilling, the flow will be from shale into wellbore.

The second and most important interaction is the diffusion flow. In diffusion flow, the movements of water molecules and ions occur due to concentration gradient. The flow of water molecules can be either into or out of the shale, depending upon the relative water activity of drilling fluid to shale. If the shale act as a perfect semi-permeable membrane than only water molecules will flow into or out of the shale [4].

The convective and diffusive movement of water molecules and ions into shale can cause clay swelling and elevation in pore pressure in shale. An increase in the pore pressure around the wellbore can cause reduction in wellbore stability by effectively weakening the rock strength. The increase in pore pressure also reduces the shear strength by reducing the mean effective stress.

Oil base mud or synthetic base mud can be used instead of water base mud to overcome the problem caused by the interaction of shale and water base mud. The interaction between the oil/synthetic base muds with shale is much simpler than that of water base mud and shale.

The oil/synthetic base muds developed the capillary pressure at the interface, these capillary forces prevents the hydraulic flow into the shale even at significant overbalance pressures. Thus keep the wellbore pressure higher than the pore pressure. Also, with stable emulsion, the internal water phase not come in direct contact with shale and a perfect semi-permeable membrane exist. This semi-permeable membrane only allow the water molecules to flow into or out of the shale [11].

Despite the significance of oil/synthetic-base muds, the use of oil/synthetic-base mud is very expensive and restricted worldwide due to their hazardous effects on environment [4]. Therefore, it is the necessity of oil industry to improve the performance of water-base mud and make the use of water-base mud more economical and environmental friendly [2, 8].

1.3. Objective

The main objective of this thesis is;

- To study the osmotic and swelling pressures as a function of stress for shale.
- To observe the effect of diffusion and chemical osmosis during shale-fluid interaction.
- To analyze the impact of confining and fluid pressure on pore pressure.

- To examine the effect of confining pressure and fluid type on shale swelling.
- To measure the capillary threshold pressure of non-wetting through shale.
- To compare the results of standard approach with other capillary threshold pressure approaches

1.4. Structure of the Report

This thesis report is organized as follow; Chapter 2 describes the causes and types of wellbore instability in shales. Chapter 3 discusses the impact of unfavorable interaction between the drilling fluid and shale. It also describes the behavior of clay mineral responsible for shale swelling. In chapter 4, a complete description of osmotic pressure and efficiency of shale membrane is given. It also includes an overview of previous work on the measurement of pore pressure during shale-fluid interaction. Chapter 5 describes the phenomena of capillary breakthrough in shale. It also discusses the different laboratory measurement methods of capillary threshold pressure. Chapter 6 explains the experimental procedure of capillary threshold pressure measurement through shales. Finally chapter 7 is about the results and discussion, followed by conclusions and recommendations.

Chapter 02
Wellbore Stability

The balance between the rock strength and the in-situ stresses around the wellbore, and the equilibrium between pore fluid and sediments affected after drilling a hole in the formation. This can results in wellbore instability in shale.

Wellbore instability in shale is mostly experienced due to [12];

i. Mechanical instability
ii. Chemical instability.

Mechanical related wellbore instability is governed by stresses around the wellbore. Mechanical instability is related to the tangential stress acting around the circumference of the wellbore, radial stress that acts along the radius of the wellbore, and vertical stress acting parallel to the well path [7]. The tangential and radial stresses are governed by mud pressure while vertical stress is produced by the overburden pressure. The overburden pressure results in vertical compression/deformation, which create compressional stresses in the horizontal direction.

The chemical related instability of the wellbore is related to complex time dependent physico-chemical interaction of water with shale. The time dependency is related to the time taken by water to flow into the shale. Figure 1 show the different wellbore instability problem which can occur during drilling.

2.1. Mechanical Instability

The stresses exist within the formation are in a state of equilibrium, before drilling of a wellbore [7]. The stresses in the removed material are transferred to the remaining formation, when the wellbore is drilled. The stresses around the wellbore are redistributed and the support offered by the drilled out rock is replaced by the hydraulic pressure of the mud. This may result in the shear stresses in the formation material exceeding its strength, leading to stress-induced wellbore failure [5].

Mechanical instability can be classified into two groups;

i. Tensile Failure
ii. Shear/Compressive Failure

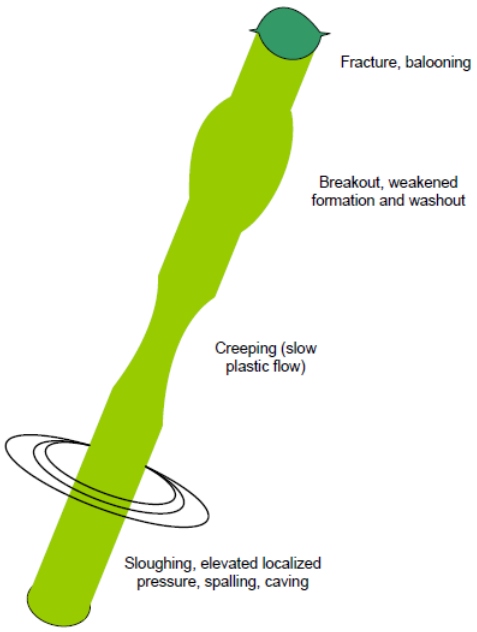

Figure 1: Possible wellbore instabilities problems during drilling [12]

2.1.1. Tensile Failure

Tensile failure occur when the effective tensile stress across the rock excessed its tensile strength [13]. The tensile failure causes the fractures in the rock which may cause the rock to break and fail, as shown in the Figure 2.

The failure criterion of tensile failure occur is given as [13];

$$\sigma^{eff} = -T_o \tag{2.1}$$

where

σ^{eff} = effective stress

T_o = tensile strength

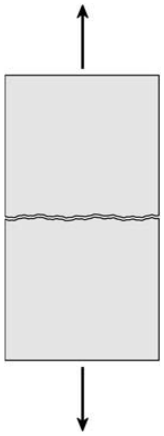

Figure 2: Tensile failure [13]

The tensile failure generally occurs when the mud density of the drilling mud is too high during drilling. The hydrostatic pressure of the drilling fluid exceeds the formation fracture pressure and cause the formation to start fracturing and result in lost circulation and well control problem. The well control problem in extreme case can lead into a kick or well blowout.

Tensile failure can be prevented by not letting the tangential stress to the limit point that it become tensile and exceeds the tensile strength of the rock [7].

2.1.2. Shear Failure

Shear failure occur when the shear stress in the rock exceeds its shear strength. This results in the development of a fault zone along the rock, which will move the two sides of the planes relative to each other in a frictional process [13], as shown in Figure 3.

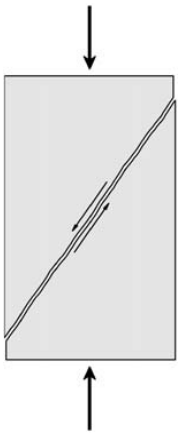

Figure 3: Shear failure [13]

Shear failure occur during drilling when the mud density of the drilling mud is too low. The formation starts to collapse due to excessively low wellbore pressure, when the hydrostatic pressure of the drilling fluid drops below the formation pore pressure. The hole enlargement, caving, breakout or even total collapse of wellbore can occur in extreme situations.

The shear failure can be prevented by minimizing the shear stress below the shear strength failure envelope. The shear stress state can be obtained from the difference between the stress components (hoop stress usually largest and radial stress usually smallest).

Generally, the mechanical stresses encounter during drilling process are [2];

- the in-situ vertical stress (overburden) and resulting horizontal stresses.
- the Pore Pressure
- the stress acting at inter-granular contact points, e.g. cohesive forces

The mud weight is important factor to deal with the mechanical instability problem. The mud weight is normally kept between fracture pressure (upper boundary) and pore pressure (lower boundary) to keep the wellbore stable, which is known as mud weigh window. Figure 4 show a typical mud weight window, from left to right the full and dotted lines are; overburden gradient (v), fracture gradient (f), minimum horizontal stress gradient (h), mud weigh gradient (m), pore pressure gradient (p) and collapsed gradient (c).

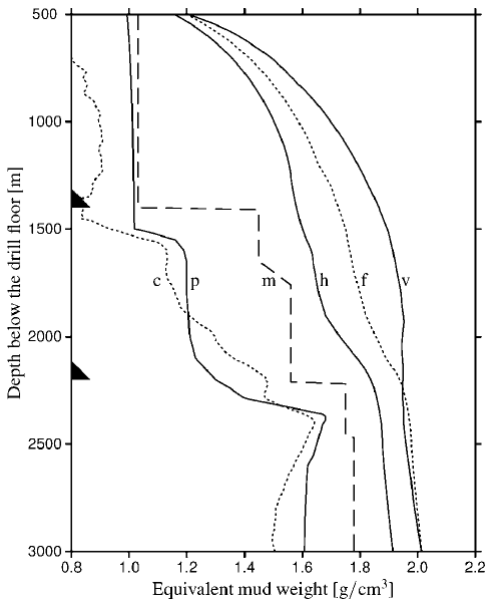

Figure 4: Mud weight window [13]

The increase in the mud weight above the fracture pressure will cause tensile failure. This will initiate the fracture in the formation which leads to the lost circulation and serious well control problems.

The formation will experience shear failure resulting from high tangential stress by lowering the mud weight below the pore pressure. The hard and brittle shale formation will splinter under compressional stress and form cave by collapsing into the wellbore. This causes hole enlargement and inadequate cleaning can lead to the bridging of the wellbore.

The excessive overburden pressure will drive the formation into the wellbore in soft and ductile shale. This results into under-gauge wellbore. Figure 5 shows the instabilities caused by shear and tensile failure in shale formation.

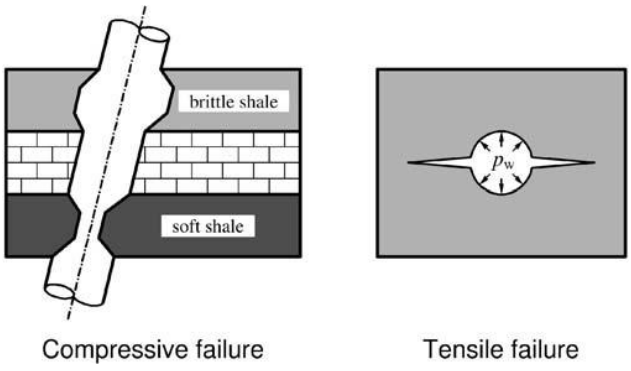

Figure 5: Shear and tensile failure in shale [13]

Mechanical instability depends upon rock strength, wellbore trajectory, bedding plane, pore pressure and hydrostatic pressure of drilling fluid. It is also related to in-situ stresses in the formation; historical tectonic activity in the area [13].

2.2. Chemical Instability

Shales are low permeable fine-grained sedimentary rocks and comprise of laminated structure made of thin layers. Shales contain large amount of clay mineral and the type and amount of clay content control the shales affinity for water. The shale reacts strongly with water because clay minerals contains negative charge and attract polar water. Shale containing smectite has a greater affinity for water than shale containing illite, mica, chlorite, zeonites or kaolinite.

Shales are low permeable but highly porous rocks and normally saturated with formation water. The overbalanced drilling with water-base mud through shale formation allows high pressure drilling fluid to flow into the formation. The low permeable nature of shale will not allow the formation of filter cake at the face of the shale. In the absence of filter cake, the drilling fluid will penetrate into the shale. The invasion of even small volume of mud filtrate into the formation causes a considerable increase in pore pressure around the wellbore. This increase in pore pressure reduces the effective mud support, which leads to the instability of the wellbore [13].

The effect of increased pore pressure, around the wellbore in shale, on wellbore stability can be describe by the Mohr's Circle [13].

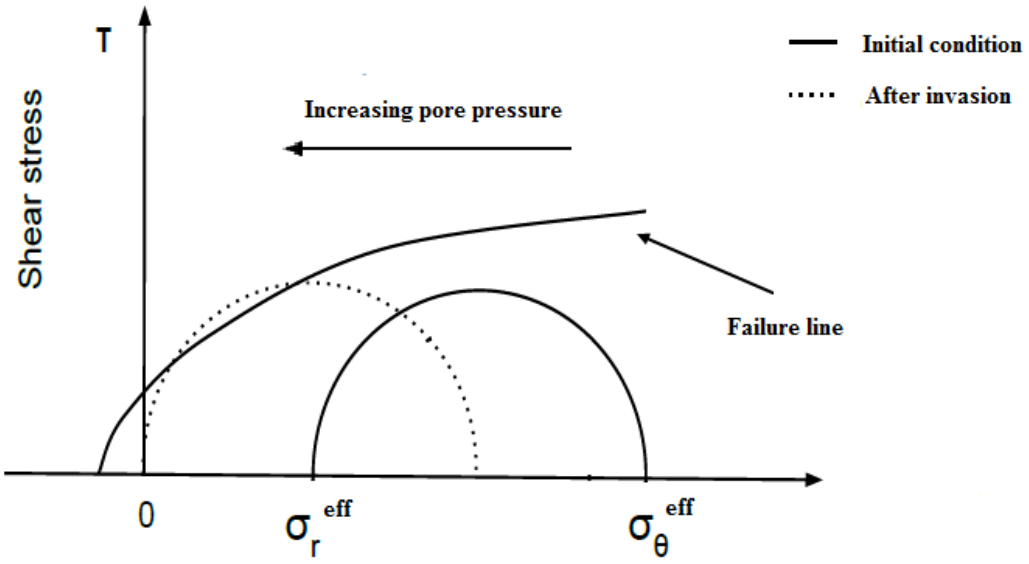

Figure 6: Mohr circle and failure lines; the effect of increasing pore pressure [13]

The effective stresses around the wellbore can be expressed by following equations [2];

$$\sigma_r^{eff} = P_w - P_{shale} \tag{2.2}$$

and

$$\sigma_\theta^{eff} = 2\sigma_h - P_w - P_{shale} \tag{2.3}$$

where

σ_r^{eff} = effective radial stress

σ_θ^{eff} = effective tangantial stress

σ_h = minimum horizontal stress

P_{well} = wellbore pressure

P_{shale} = pore pressure of shale

The pore pressure will increase when the drilling fluid penetrates in the formation, and after passage of time the pore pressure will become equal to the wellbore pressure. The effective stresses than becomes;

$$\sigma_r^{eff} = 0 \tag{2.4}$$

and

$$\sigma_\theta^{eff} = 2\sigma_h - 2P_w \tag{2.5}$$

Equation 2.4 shows that an increase in pore pressure decreases the effective stresses, and the circle, moves toward left and cross the shear-tensile failure line, as shown in Figure 6. Thus, increase pore pressure may destabilize the formation with respect to shear and tensile failure.

The rate and the magnitude of increase in pore pressure depend primarily upon viscosity and adhesion properties of drilling fluid and the petro-physical properties of shale [2].

Chapter 03
Shale-Fluid Interaction

The properties of shale ranges from very soft to hard, and from very laminated to very compact. Shale destabilizes when drilling fluid penetrate existing fissures, fractures and weak bedding planes.

The factor that distinguishes shale from other sedimentary rocks is its sensitivity to the water phase of drilling fluids. The interaction between shale and water will decrease the strength of the shale with time and making it more prone to mechanical/chemical stability failure.

In addition to the fluid invasion, the unfavorable shale-fluid interaction will also alter the pore pressure or effective stress state [10].

3.1. Fundamentals of Shale Behavior

The forces acting on shale, containing clay and other minerals, can be divided into mechanical and physio-chemical forces [2]. The mechanical forces include [2];

- the in-situ vertical stress (overburden) and resulting horizontal stresses.
- the pore pressure
- the stress acting at inter-granular contact points, e.g. cohesive forces

and, the phsico-chemical forces acting on clay minerals are [2];

- the van der Waal attraction
- the electrostatic Born repulsion
- short-range repulsive and attractive forces that are derived from hydration/solvation of clay surface and the ions that are present in the interlayer spacing (free or absorbed)

The van der Waals forces are the electrical forces produce because of the electrical movement within the clay units. These forces exist in clay minerals due to the nonsymmetrical distribution of electrons in the silicate crystal and act as dipoles. These dipoles have the tendency to attract other dipoles like water molecules [7]. Last two forces are usually lumped together to form the hydration pressure or swelling pressure, as these two pressures are responsible for the swelling behavior of clays and shale [2]. Figure 7 show the different forces acting on a single clay platelet of shale.

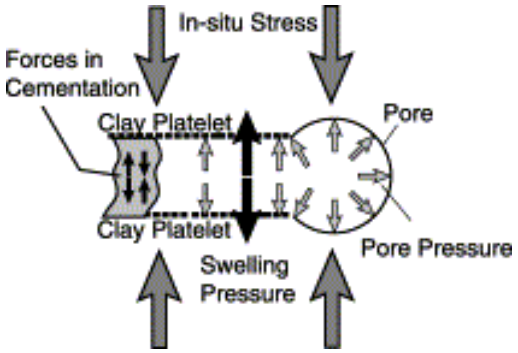

Figure 7: Downhole forces acting on a single clay platelet of shale [2]

3.1.1. Shale Swelling

The interaction of shale with water-base mud not only cause the reduction in shale strength by increase in shale pore pressure Also, the movement of water into the shale can cause shale swelling which may lead to the instability or failure of the wellbore.

Swelling occurs in shale due to the interaction of pore water with clay minerals. Clay minerals are small in size but having large reactive surface area. Clay minerals contain negative charge and have great affinity to attract and adsorb water, which present in the pores of the shale. Clay minerals, such as smectite and illiites, have the tendency to expand up to 20 times to its original volume by adsorbing water in between their cells.

There are two types of clays swelling, which are mostly observed in shale [7];

i. Inter-crystalline swelling
ii. Osmotic swelling

In inter-crystalline swelling, the hydration of clay by cations exchange is the source of inter-crystalline swelling. The ions concentration difference between clay and pore water results in osmotic swelling [7].

3.1.2. Classification of the Clay Minerals

Clay minerals are generally classified into three categories based on their expanding capability [14], such as :

i. Non-expansive
ii. Moderately expansive
iii. Highly expansive

The kaolinite and illite minerals come in the category of non-expansive clay minerals, vermiculite are moderately expansive minerals, and monmorillonite fall in the category of highly expansive clay minerals.

The volume change in minerals defines the degree of swelling in clay. High volume change in clay minerals indicates high clay swelling and small change in volume represents low clay swelling. Table 1 presents the relationship between particle size of clay mineral and their observed volume change when come in contact with water molecules.

Table 1: Classification of clay minerals [14]

Mineral	Average particle thickness (nm)	Average specific surface area (m^2/g)	Observed volume change
Montmorillonite	2	700 – 800	High
Illite	20	80 – 120	Medium
Kaolinite	100	10 - 15	Low

The size of montmorillonite clay mineral is much smaller as compared to the other clay minerals, such as illite and kaolinite. However, the montmorillonite mineral shows high volume change which ultimately results in high degree of clay swelling. This large volume change in montmorillonite is due to its large surface area, which permit more water molecules and other cation to attach on the surface area of montmorillonite than any other clay minerals.

3.2. Transport Mechanisms in Shale

Drilling through a shale formation with a water based mud can result in two types of flow, between the shale and drilling fluid [4], these are;

i. Hydraulic flow
ii. Diffusion flow

3.2.1. Hydraulic Flow

The hydraulic flow is the simple flow of water molecules which occur between drilling fluid and shale [4]. The hydraulic flow is based on Darcy's law [4];

$$q = -\frac{k\,A}{\mu}\frac{(P_{mud} - P_{shales})}{L} \tag{3.1}$$

where

q = flow rate

k = permeability

A = cross-sectional area of shale

μ = viscosity of drilling fluid

P_{mud} = hydrostatic pressure of drilling mud

P_{shale} = pore pressure of shale

L = length of shale

In hydraulic flow, the fluid will flow between the wellbore and shale due to pressure gradient between the drilling fluid and shale. In overbalance drilling, where wellbore pressure is high than the shale pore pressure, the fluid flow will be from wellbore into the shale. In underbalance drilling, the flow will be from shale into the wellbore.

The sandstone contains significant amount of permeability. Therefore the fluid influx into the sandstone is sufficient to form a filter cake at the face of the sandstone and prevents further fluid loss in the formation. However in shale, the filter cake cannot develop as the permeability of typical shale is much less than that of filter cake. Also, the particle size of a typical filter cake is too large to plug the pore throats of shale.

3.2.2. Diffusion Flow

The second and most important flow between the shale and the drilling fluid is the Diffusion flow. Diffusion flow is based on the Flick's law [6];

$$J = -D\left(\frac{C_{shale} - C_{mud}}{\Delta x}\right) \tag{3.2}$$

where

J = diffusion flux

D = diffusion coefficient

C_{shale} = concentrations of ions in shale

C_{mud} = concentrations of ions in mud

Δx = length of shale

The movements of water molecules and ions between drilling fluid and shale due to concentration gradient, is called diffusion flow. The movements of water molecules and ions can be either into the shale or out of the shale and it depends upon [8, 9];

- relative activity of drilling fluid to the shale activity (affects water movement)
- relative concentration of the ions (affects ion movement)
- interaction between water/ions and clay minerals
- restrictions to water or ions movements (depends upon membrane permeability)

The movement of ions either into or out of shale can be determined from the equation 3.2 [6];

i. $C_{shale} < C_{mud}$, the flow of ions will occur into shale

ii. $C_{shale} > C_{mud}$, the flow of ions will occur out of shale

iii. $C_{shale} = C_{mud}$, no flow will occur.

In case of shale acting as a perfect semi-permeable membrane, only water molecules will flow into or out of the shale [8].

The convective and diffusive movement of water molecules and ions into shale can cause clay swelling and change in pore pressure in shale. An increase in the pore pressure around the wellbore can cause reduction in wellbore stability by effectively weakening the rock, because the increase in pore pressure will reduce the shear strength by reducing the mean effective stress. Table 2 shows the transport mechanisms which occur in shale.

Table 2: Potential transport mechanism in shale [9]

Mechanism	Driving force	Molecular species
Hydraulic flow	Hydraulic pressure difference (Mud weight – Pore pressure)	Bulk water (cations, anions and water into or out of shale)
Diffusion flow	Chemical potential of ions and water molecules	Ions and water molecules into or out of Shale
Chemical osmosis	Chemical potential of water	Water into or out of shale
Reverse osmosis	Hydraulic pressure	H_2 into or out of Shale

3.3. Chemical Osmosis

Chemical osmosis is the movement of water molecules, through semi-permeable membrane, from low solute concentration to high solute concentration, until the concentration of solute come in equilibrium state.

Chemical Osmosis is caused by the difference in solute concentration between the water phase of drilling fluid and the shale pore water. The solute imbalance is separated by shale which acts as a semi-permeable membrane and only allows the flow of water molecules. Water moves from low solute concentration to high solute concentration until the balance is achieved.

Water molecules moves into the shale and increase the pore pressure, if the solute concentration in drilling fluid is too low. Whereas, if the solute concentration in the drilling fluid is too high, the pore water in shale will flows into the wellbore and cause the dehydration of the shale.

In shale/water base mud system, the perfect semi-permeable membrane does not exist. However the system obtains the membrane efficiency to some degree and sustains the osmotic flow, if the concentration difference between solute and solvent exist.

The driving force in the chemical osmosis can be determined by the taking the difference of water activity between drilling fluid and pore water present in shale at in-situ conditions. The flow will always take place from high water activity to low water activity [15].

3.4. Pressure Diffusion

Pressure diffusion is the change in pressure around the wellbore with time, when the drilling fluid at high wellbore pressure come in contact with the pore fluid [7].

In overbalance drilling, the wellbore pressure is much higher than the pore pressure at initial conditions. This allows the drilling fluid to compress the pore fluid at wellbore wall. The pore pressure around the wellbore varies with time until a steady state pressure distribution around the wellbore is reached [7]. Figure 8 shows the development of pressure front along with filtrate and solute invasion fonts with time around the wellbore in shale.

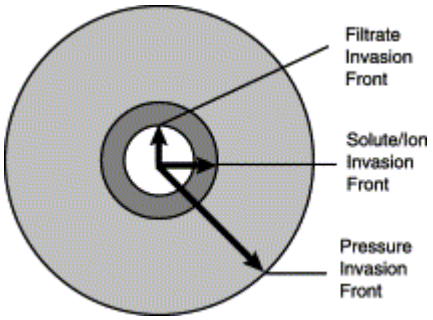

Figure 8: Development of various fronts around a wellbore in shale [2]

The permeability of shale is relativity low; therefore it may takes from few hours to days or week for increase and dissipation of excess pore pressure. This will result in the pressure loss and reduction in the effective stress and results in wellbore instability [7].

The diffusion coefficient, also called consolidation coefficient, is the measure of how long the disturbance of pore pressure can propagates for a given time [13]. By assuming $K_{fr}, G_{fr} \ll K_s$, the diffusion constant can be determined from the given equation [13];

$$C_D \approx \frac{kK_f}{\eta_f \emptyset}\left[1 + \frac{K_f}{\emptyset\left(K_{fr} + \frac{4}{3}G_{fr}\right)}\right]^{-1} \tag{3.3}$$

where

C_D = pore pressure diffusion constant

k = permeability

K_f = bulk modulus of fluid

η_f = fluid viscosity

$\emptyset$ = porosity

K_{fr} = drained bulk modulus

G_{fr} = shear modulus of the frame

The relationship between length, time and diffusion constant is given as [13];

$$l_D^2 = C_D \tau_D \tag{3.4}$$

where

l_D = diffusion length

C_D = pore pressure diffusion constant

τ_D = diffusion time

Chapter 04
Osmotic Pressure

4.1. Introduction

Osmosis is the flow of water molecules into or out of the shale through semi-permeable membrane due to difference in chemical potential. This potential difference causes the flow of water between drilling fluid and shale, through semi-permeable membrane. The flow will be from low solute concentration to high solute concentration, until the concentration of solute come in equilibrium state [11]. The process cause an elevation in pressure at high solute concentration side, this increase in pressure is called osmotic pressure [8], as shown in Figure 9.

Shale acts as membrane and control the flow of ions and water molecules between drilling fluid and shale. If shale acts as a perfect semi-permeable membrane, it hinders the movement of ion. The restriction of ion flow will lead to imbalance between the solute concentrations. This will cause an osmotic pressure difference, which act as driving force for movement of water molecules across the drilling fluid and shale [9].

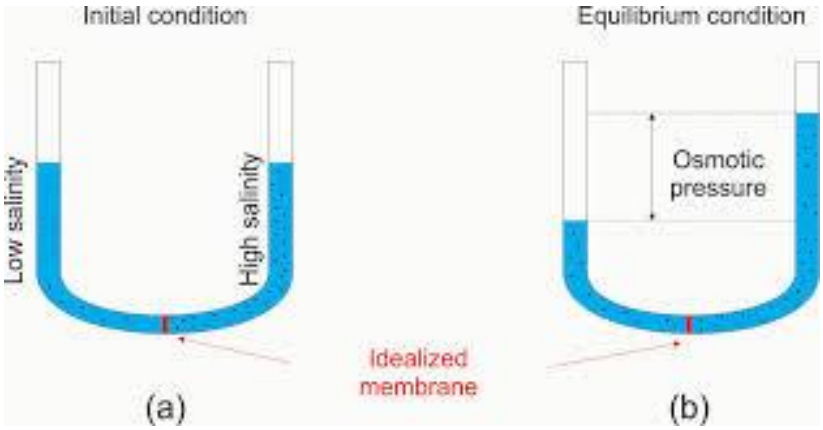

Figure 9: Osmotic pressure: (a) initial condition, (b) equilibrium condition [16]

A low water activity arises in drilling fluid having high ion concentrations, which cause a difference in osmotic pressure between drilling fluid and shale. This osmotic pressure difference cause the flow of water molecules from shale having low ion concentration and high water activity, to drilling fluid having high ion concentration and low water activity [17].

In case of shale with high ion concentration and drilling fluid with low ion concentration, shale exhibit low water activity and water molecules flow from drilling fluid towards shale [17].

The flow of water molecules between drilling fluid and shale continues until the water activity of drilling fluid will equal to the water activity of shale. When the water activity of both drilling fluid and shale equals to each to each other, the difference in osmotic pressure become zero and further movements of water molecules stops [17].

The water activity is a good indicter for indication of hydration state of shale and the potential of shale to absorb water. The concept of water activity in shale was introduced by Chenevert and Pernot [5]. The water activity of shale can be defined as, the ratio of vapor pressure of shale pore fluid and vapor pressure of pure water and can be expressed mathematically as [6];

$$a_{w,shale} \cong \frac{P_{shale}}{P_w} \tag{4.1}$$

where

$a_{w,shale}$ = water activity of shale

P_{shale} = vapor pressure of shale

P_w = vapor pressure of pure water

The water activity of pure water is 1, as in pure water all molecules move freely and not bounded electrostatically to any salt ion. The water activity reduces with an increase in salt concentration. The water activity of shale is always less than 1 ($0 < a_{w,shale} < 1$).

Shale acts as a membrane and control the flow of ions and water molecules between drilling fluid and shale. Chemical Osmosis occur when shale act as a perfect semi-permeable membrane, it hinders the movement of ions and only allow the flow of water molecules [8].

Low and Anderson (1958) derived an equation to calculate osmotic pressure across a semi-permeable membrane [6, 18];

$$\Delta\Pi = \frac{R\,T}{\bar{V}_w} ln\left(\frac{a_{w,shale}}{a_{w,mud}}\right) \tag{4.2}$$

In actual downhole conditions, when shale come in contact with drilling fluid, it does not act as a perfect semi-permeable membrane and the pressure difference measured is less than the

predicted theoretical osmotic pressure [6]. Therefore, membrane efficiency (α_m), also called reflection coefficient, was introduced to correct the leaky or non-ideal state of shale membrane [6, 19]. The above equation than becomes;

$$\Delta P = \alpha_m \frac{R\,T}{\bar{V}_w} ln\left(\frac{a_{w,shale}}{a_{w,mud}}\right) \tag{4.3}$$

and

$$\alpha_m \cong \frac{\Delta P}{\Delta \Pi} \tag{4.4}$$

where

$\Delta\Pi$ = osmotic pressure difference

ΔP = pressure difference

α_m = membrane efficiency

R = gas constant

T = absolute temperature

$\bar{V}_w$ = molar volume of water

$a_{w,shale}$ = water activity of shale pore fluid

$a_{w,mud}$ = water activity of drilling mud

Based on the Equation 4.3, following circumstances can happen [6];

i. $a_{w,shale} < a_{w,mud}$, the water molecules flow from drilling fluid into shale, which increases the water content in shale pores and lead to an increase in pore pressure around the wellbore.

ii. $a_{w,shale} = a_{w,mud}$, no flow take place across drilling fluid and shale.

iii. $a_{w,shale} > a_{w,mud}$, The water molecules flow out of shale, which lower the water content in shale pore spaces and reduce pore pressure around the wellbore.

4.2. Membrane Efficiency of Shale

The membrane efficiency of shale basically defines the capability of shale to restrict the flow of ions across drilling fluid and shale [18]. When shale acts as perfect semi-permeable

membrane, it completely hinders the flow of ions. Whereas, if shale completely allow the movements of ions, the shale act as non-selective membrane [18].

The membrane efficiency of shale can be define mathematically as [18];

$$\alpha_m = 1 - \frac{v_s}{v_w} \tag{4.5}$$

where

α_m = membrane efficiency

v_s = mobility of solute (ions)

v_w = mobility of water

From the above equation it is clear that, if $v_s = 0$ and $v_w \neq 0$, the movements of ions are completely restricted and only water molecules have free mobility across drilling fluid and shale. This indicates that shale acts as an ideal or perfect semi-permeable membrane, having membrane efficiency of unity (α_m = 1).

If $v_s = v_w$, the ions and waters molecules have equal mobility and shale act as non-selective membrane with membrane efficiency of zero (α_m = 0).

The case in which the flow of ions are not completely restricted and the mobility of ions are less than that mobility of water molecules $v_s < v_w$, the shale acts as leaky or non-ideal membrane ($o < \alpha_m < 1$) [18].

van Oort, Hale [1] performed pressure transmission tests to measure the membrane efficiency of shale and found that the membrane efficiency depends on characteristics of both shale and fluid. The test results showed that membrane efficiency is influenced by solute size, pore throat radius, cation exchange capacity and surface area.

The membrane efficiency increases with an increase in clay content surface area and ratio of solute size to radius of pore throat, and also increase with reduction in shale permeability. The membrane efficiency of shale was very low and range between 1 to 10 % [20].

4.3. Overview on Previous Work

Mody and Hale [9] were the first who measure the pore pressure changes in shale due to shale-fluid interaction. They designed and used special equipment called oedometer, in order to

provide axial and radial stress around the shale sample and detect any changes in pore pressure due to water activity between shale and frilling fluid.

Van Oort, Hale [18] were the next who design the pressure transmission test to measure and quantify the parameter affecting the fluid transportation between shale and drilling fluid and their impact on the change in pores pressure under downhole condition. Figure 10 show the geometry of oedometer and pressures transmission test apparatus.

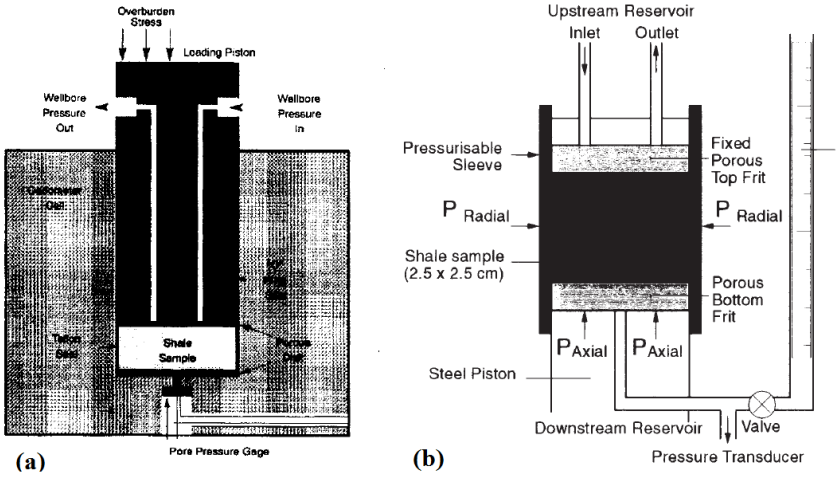

Figure 10: Schematic; (a) oedometer, (b) pressures transmission apparatus [9, 18]

Muniz, da Fontoura [21] design a diffusion cell to analyses the effect of shale-fluid interaction by applying hydraulic and chemical gradient through shale sample. In addition to this, they also measure the cation exchange capacity and membrane efficiency.

The procedure adopted for the measurement was to first saturate the sample with simulated fluid. The contact of sample with any fluid including simulated pore fluid can alter the properties of the sample because the sample comes in contact with bulk fluid during saturation. While in downhole conditions the sample is surrounded by more shale.

Ewy and Stankovic [4], [11, 19] came up with the idea to preserve the sample and measure the changes in pore pressure with saturation at in-situ conditions. Table 3 shows a comparison of tests perform by different authors in order to measure osmotic pressure.

Table 3: Comparison of osmotic test results [1, 4, 21]

Author	Shale	Permeability (nD)	Drilling fluid	Shale activity	Water activity	Pressure difference (MPa)
Ewy and Stankovic	N1	2-4	23.2% NaCl	0.96	0.8	0.6
			31.7% $CaCl_2$		0.6	2.3
	A2	4-8	23.2% NaCl	0.75	0.8	1,3
			31.7% $CaCl_2$		0.6	1.9
Muniz and Fontoura	30	38.5	15% $CaCl_2$	0.96	0.93	0.5
	31	60.8	25% $CaCl_2$	0.96	0.78	1.0
	32	81.0	35% $CaCl_2$	0.96	0.5	0.2
Van Oort and Hale	-	0.61	35% $CaCl_2$	0.84	0.51	1.5
	-	1.5	26% KCl	0.84	0.84	0.5
	-	1.5	16% $Al_2(SO_4)_3$	0.86	0.89	1.7

Ewy and Stankovic [4] and Muniz, Fontoura [3] conclude that increase in salt concentration help in extracting more water from shale. Also increasing the confining pressure helps in controlling the shale swelling.

Chapter 05
Capillary Threshold Pressure in Shale

Drilling through shale formation with oil base mud developed capillary pressure at the interface of oil base mud and pore water due to small pore throat radius and high interfacial tension. This capillary pressure in the shale prevent the oil based mud from entering into the formation because of the lower pressure than the capillary threshold pressure, and thus, allow to keep the wellbore pressure sufficiently higher than the pore pressure.

However, if the pressure difference between wellbore pressure and pore pressure will be much high, the wellbore pressure may reach the capillary threshold pressure and allow the mud to enter into the formation, which lead to the instability of the wellbore.

5.1. Capillary Threshold Pressure

The capillary threshold pressure is the pressure required for non-wetting phase (oil or gas), to displace the wetting phase (brine) in the largest port throats of a water-wet formation [22].

An interfacial tension develops at the interfaces, when two immiscible fluid come in contact with each other, such as water as a wetting phase come in contact with oil as non-wetting phase. A difference in pressure between these two immiscible fluids will occur across a curved interface at equilibrium, this pressure difference is called capillary pressure [23].

Capillary threshold pressure is achieved when the capillary pressure is high enough, so that non-wetting phase start displacing wetting phase, and can be mathematically expressed as [23];

$$P_c = P_{nw} - P_w \tag{5.1}$$

or

$$P_c = 2\sigma \frac{cos\theta}{r} \tag{5.2}$$

where

P_c = capillary threshold pressure

P_{nw} = pressure of non-wetting phase

P_w = pressure of wetting phase

σ = interfacial tension between non-wetting and wetting phase

θ = contact angle

r = pore throat radius

5.2. Capillary Breakthrough

The process of capillary breakthrough in porous medium takes place in several phases. In the first phase, when the pressure of the non-wetting phase exceed the capillary threshold pressure, the non-wetting phase start displacing wetting phase and form a continuous flow path. In this stage, the non-wetting phase will only fill the large interconnected pores, as the large pores has less resistance to the capillary threshold pressure. Also, at this point, the non-wetting phase will be limited to a small portion of large interconnected pores.

In the second phase, when the pressure of non-wetting phase will further increases, the non-wetting phase will start displacing wetting phase from small pores and form additional flow paths in the system. The divergence in the flow paths will now increase and the flow will be now less focused. The formation of additional flow paths will increase the saturation and relative permeability of non-wetting phase. Also, the flow regime will be shifted to viscous dominated from capillary dominated. However, the pressure of the non-wetting phase will increase in this stage and become higher than the capillary threshold pressure, but will be still less than the capillary breakthrough pressure ($P_c < P_{c,entry} < P_{c,threshold}$).

In the third phase, the further increase in the pressure of non-wetting phase form a continuous flow path which consists of large pore throat diameter, which are interconnected with each other, throughout the system. The pressure of non-wetting phase will reach to the threshold pressure in this stage. The different stages of capillary breakthrough process can be shown in Figure 11.

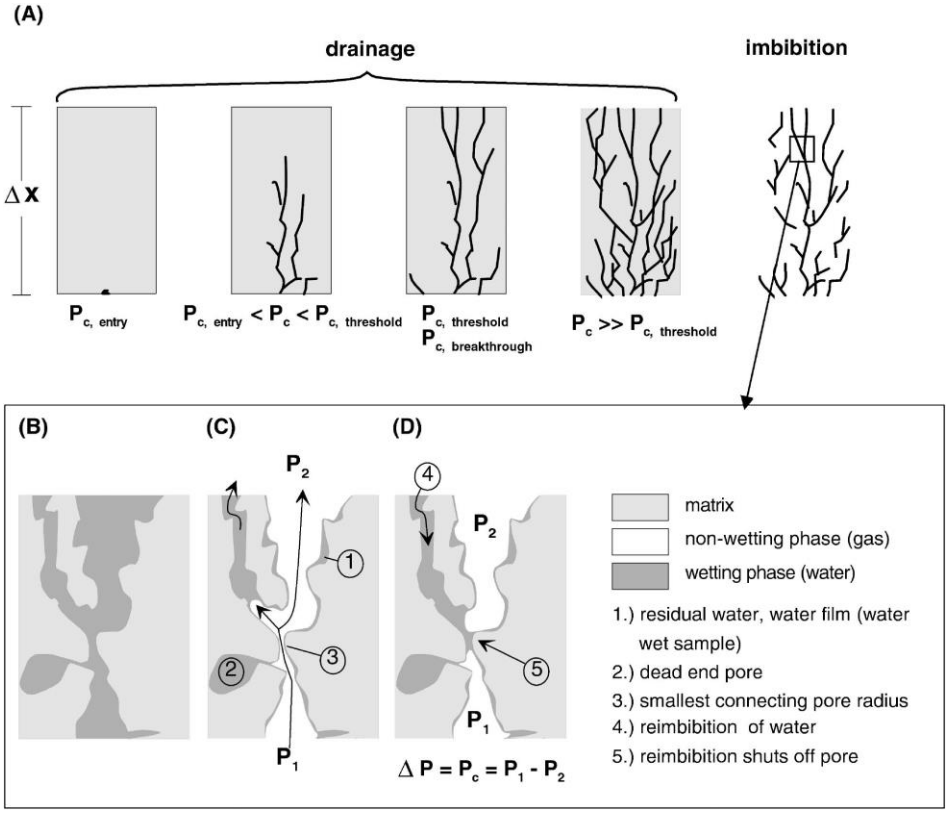

Figure 11: Stages of capillary breakthrough process in fine-grained rocks [24]

After reaching the breakthrough pressure, the excess pressure of non-wetting phase will be reduced and the re-imbibition process of wetting phase will start taking place. In this phase, the wetting phase will start displacing the non-wetting phase first from small pores and later from larger pores. The continuous re-imbibition of wetting phase will reduce the relative permeability of non-wetting phase by blocking the interconnected flow paths.

5.3. Impact of Interfacial Tension, Contact Angle and Pore Throat Radius on Capillary Breakthrough

The capillary threshold pressure is greatly affected by interfacial tension between the wetting and non-wetting phase, contact angle between pore and fluid, and size or radius of the pore throats.

i. Interfacial Tension

Interfacial tension is the contractile force per unit length that exists at the interface of two immiscible fluids such as oil/gas and water.

The capillary threshold pressure is directly proportional to the interfacial tension, as shown in equation 4.1. The interfacial tension is affected by temperature, pressure and composition of each phase.

ii. Contact Angle

The angle at which two immiscible fluid come in contact with each other at solid surface, is called contact angle (θ).

The contact angle is inversely proportional to the capillary threshold pressure. Hence, lower the contact angle, higher will be the capillary threshold pressure. The small contact angle indicates strong water wet nature of the shale. The composition of the rock minerals largely affects the contact angle.

iii. Pore Throat Radius

The size of the pore throat is also inversely proportional to the capillary threshold pressure. Therefore, smaller the pore throats higher will the capillary threshold pressure. The resistance for non-wetting phase to displace wetting phase is much higher in small pore throat as compare to that in large pore throats.

5.4. Measurement Method for Capillary Threshold Pressure

The capillary threshold pressure can be measured in two ways, either by core measurement in laboratory or from log data by using empirical modeling [22].

The existing laboratory measurement methods for capillary threshold pressure in shale are;

i. Mercury porosimetry
ii. The continuous injection approach
iii. The residual pressure approach
iv. The standard approach (step-by-step approach)

5.4.1. Mercury Porosimetry

The mercury porosimetry is the most simplest and time efficient approach for the measurement of capillary threshold pressure. The mercury porosimetery approach drive the capillary threshold pressure value from mercury porosimetery curve, by knowing the values of interfacial tension and contact angle between fluid system and rock [25]. Figure 12 shows the result of capillary threshold pressure obtain from mercury porosimetery.

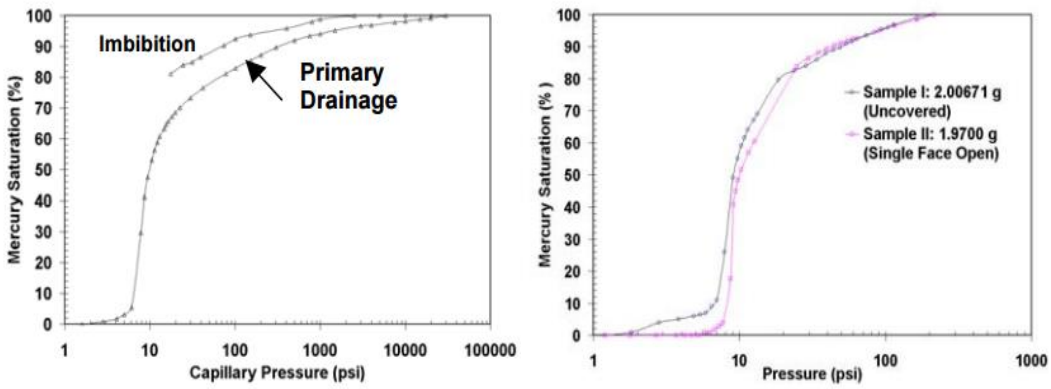

Figure 12: Mercury porosimetry results [26]

The main advantage of mercury porosimetry over other measurement method is its simplicity and quickness [25]. In addition to these advantages, there are some weaknesses of this approach. The first drawback of this approach is absence of confining pressure, the confining pressure represent as the horizontal stress around the wellbore. The petrophysical properties, especially permeability, of shale are sensitive to confining pressure. The permeability of shale reduces with an increase in overburden pressure.

Another disadvantage of this method is the use of dry sample for the test. The drying of sample change the properties and pore structure of shale [27].

5.4.2. The Continuous Injection Approach

The continuous injection approach is based on the constant injection of now-wetting phase with very small flow rate. In the first phase, the pressure of the non-wetting phase at inlet is increase gradually and consciously until the pressure exceeds the threshold pressure of the sample. When the inlet pressure exceeds the threshold pressure, the fluid starts to flow in the sample.

The main disadvantage of this method is associated with the small flow rate. The flow with small rate neglect the viscosity gradient of water phase [25].

5.4.3. The Residual Capillary Pressure Approach

The residual capillary pressure approach was proposed by Hildenbrand, Schlömer [24] to avoid overestimation of capillary threshold pressure. This approach is based on the continuous increase in pressure of non-wetting phase at extremely small flow rate, until the capillary threshold pressure is archived. In the beginning of the test, the pressure of non-wetting phase applied at the inlet is kept adequately higher than the expected capillary threshold pressure.

The residual capillary pressure approach is much faster compared to the standard capillary pressure approach. However, the residual capillary threshold pressure approach underestimate the capillary threshold pressure value and may result in decreased value compared to the actual capillary threshold pressure value [27]. Figure 13 show the comparison between the residual and the standard approach for capillary threshold pressure measurement.

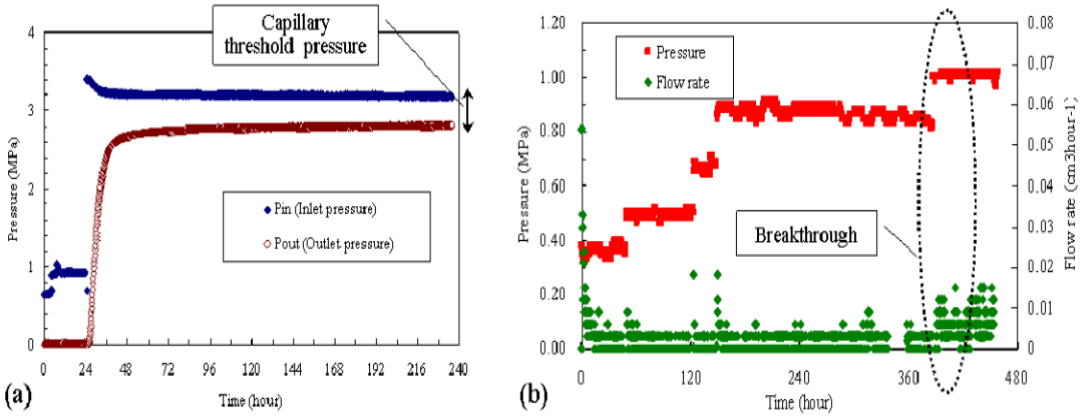

Figure 13: Comparison between residual and standard approach for same shale sample. (a) the residual approach, (b) the standard approach [28]

5.4.4. The Standard Approach (Step-by-step Approach)

The standard approach also called step-by-step approach is based on step-by-step increase in pressure of non-wetting phase at inlet and observing the changes in pressure at the outlet [22]. In this method the pressure at the inlet is raise gradually in stages until the pressure at the outlet is increases, which shows that the capillary threshold pressure is achieved. Figure 14 show the standard capillary threshold pressure measurement method by using oil-base mud for Pierre shale. The capillary threshold pressure is the difference between the upstream pressure and the downstream pressure, when the downstream pressure starts increasing.

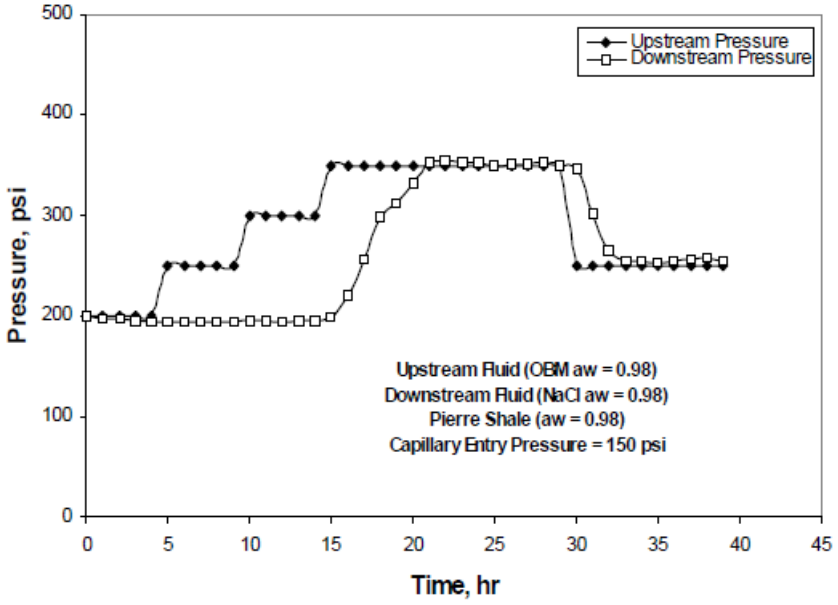

Figure 14: Test results of threshold capillary pressure using the standard approach [22]

The brine flows at very small rate from the outlet due to low permeable nature of shale, when the capillary threshold pressure will achieve. This make it very difficult to detect the presser increase at outlet accurately and may result in the overestimation of capillary threshold pressure [27]. Therefore, the accuracy of standard approach results depends upon the selection of pressure increment value and pressure step duration. The small pressure time step and too high increment in pressure can lead to overestimation of the capillary threshold pressure value.

Table 4: Comparison of different capillary threshold pressure approaches [25]

Approach	Duration	Rock Structure	In-situ	Accuracy
Mercury porosimetry	Good	Medium	Bad	Medium
Standard approach	Bad	Good	Good	Good
Continues approach	Good	Good	Good	Medium/Bad
Residual approach	Good	Good	Good	Bad

Table 4 shows the comparison between different methods for measurement of capillary threshold pressure in shale. The standard method has good accuracy of results but is more time consuming compared to other methods. The residual method is fast but least accurate.

Chapter 06

Test Procedure to Measure Threshold Capillary Pressure

6.1. Properties of Shale Sample

The samples used for the capillary threshold pressure test was outcrop of Pierre shale of marine origin and Field shale (the name and composition of field shale sample cannot be published due to confidentiality issue). The sample was preserved in mineral oil after coring, to protect from any loss of water contact due to exposure or interaction with the atmosphere or any other fluid.

The composition of the fined grained mineral present in Pierre shale was identified by the using the technique of X-ray diffraction analysis as shown in Table 5;

Table 5: Semi-quantitative mineralogical composition of the Pierre shale sample [29]

Mineral	Percentage
Smectite	31.5
Quartz	20.1
Mica/Illite	16.6
Plagioclse feldspar	15.7
Kaolinite	6.8
Chlorite	2.2
Pyrite	2.0
Calcite	1.8
Dolomite/Ankorite	1.8
Potassium feldspar	0.7
Siderite	0.7

The fluid present in the pores of the Pierre shale was brine, having water activity of 3.5 % w/w NaCl solution. Base oil was used as non-wetting fluid. The interfacial tension between the base oil and pore fluid was 0.03 N/m. Table 6 shows the summary of Pierre shale sample properties.

Table 6: Properties of Pierre shale sample [29]

Shale type	Pierre Shale
Permeability	14 nD
Porosity	22.5
Average pore throat radius	0.0245 µm
Water activity	0.98
Relative humidity	10.43
Interfacial tension	0.03 N/m or 30 mN/m
Wettability	Water wet

6.2. Sample Setup

The pressure cell was made up of stainless steel, having the capability of handling pressure up to 40 MPa. For the measurement of pressure, three pressure sensors were used. The pressure sensor P1 was used for upstream pressure, P2 for downstream pressure and P3 for confining pressure. The constant volume valve V1 was used for upstream flow and V2 for downstream flow. While valve V3 and V4 were Autoclave vales for flow of confining fluid. The valves were connected with the pressure cell through autoclave tube, having outer diameter of 3.18 mm and inner diameter of 1.32. The Quizix pumps were used for applying confining, upstream and downstream pressures. The Quizix pumps are positive displacement pump, having maximum pumping capacity of 15 ml/min.

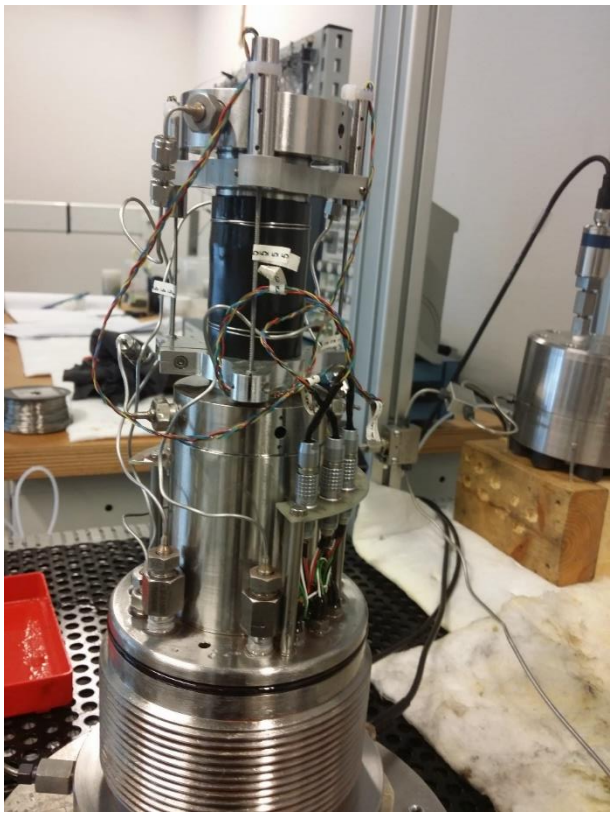

Figure 15: Exterior of pressure cell

Linear variable deformation transformers (LVDT) sensors were used, in addition to pressure sensor, to measure the axial and radial deformation of the sample during the test. The sensors were set around the sample between upper and lower piston. All the pressure and LVDT's sensor were instrumented to the computer with the Cadman software.

A porous disc was placed in the lower chamber, before installation of the sample. After placing the sample, another porous disc was placed on the top of the sample. The purpose of the porous disc was to equally apply the pressure on the top of the sample. Also, these porous discs should be immersed in the base oil and any trapped air should be removed before installation.

An elastics rubber sleeve was then enfolded around the sample and tightly wrapped with steel wire in order to avoid the contact between the confining fluid and the sample as shown in Figure 15.

Finally, the cell was closed off and filled with the base oil, which will transmit the confining pressure to the sample during consolidation process. The excess base oil and air was removed from the valve at the top of the pressure cell, as shown in Figure 16.

Figure 16: Interior of pressure cell

The sample should be installed carefully between pistons by make sure that no air would be trapped between the sample, porous disc and the piston. Also, minimize the direct contact of sample and air during placement of sample in the pressure cell.

6.3. Consolidation Phase

The consolidation phase was the first phase of the test. The consolidation phase is based on the fact that any excess pore pressure already present or generated during the consolidation phase must be dissipated before the commencement of the final phase. This is done to ensure that the sample is fully saturated and contain uniform pore pressure.

The values of confining pressure and the back pressure would be adjusted at the start of the consolidation phase. During rising of the confining pressure, the back pressure was kept constant to drain off the excess pore pressure from the sample. Since base oil was used as non-wetting in this test, therefore the dissipation of excess pore pressure should be form the downstream only. This can be done by maintaining adequate differential pressure, but make sure that the differential pressure must be less than estimated capillary threshold pressure.

The confining pressure should be increased slowly and gradually so that the increase in the pore pressure must be less than the effective differential pressure. The excessive pore pressure must have given enough time for dissipation.

The time required for pore pressure diffusion and expected capillary threshold pressure can be calculated by using Equation 3.4 and 5.2. While, the maximum rate of confining pressure can be calculated by using the following equations [29];

$$r = \frac{\Delta P}{\Delta t} < \frac{\Delta P_{max}}{\Delta t} = \frac{C_D \Delta P_{max}}{l^2} \tag{6.1}$$

where

r = maximum rate of confining pressure, MPa

ΔP = pressure difference between upstream and downstream, MPa

ΔP_{max} = maximum allowable pressure difference between upstream and downstream, MPa

Δt = time, sec

C_D = pore pressure diffusion constant, m^2/s

l = length of sample, m

6.4. Capillary Threshold Pressure Test

The standard capillary pressure approach was used in order to measure the capillary threshold pressure in shale sample by using base oil as non-wetting fluid.

6.4.1. Test Description

The standard approach also called step-by-step approach is based on step-by-step increase in pressure of non-wetting phase at inlet and observing the changes in pressure at the outlet. The accuracy of the standard approach is based on selection of pressure increment and time length for each step. The smaller the pressure increment and longer the time length, the more accurate would be the results

The time required for pressure diffusion and theoretical capillary threshold pressure values must be calculated before the commencement of capillary threshold pressure test, this has to be done to get support in the selection of pressure increment and time length for each step

The differential pressure was increased slowly and gradually in steps, during the test, until the pressure at the downstream start rising. The increase in the downstream pressure shows that the capillary threshold pressure is achieved. The difference between the upstream and downstream pressure is the capillary threshold pressure. It is suggested that, after achieving the capillary threshold pressure, the reserve flow test should be conducted by dropping the upstream pressure to analyses its effect at downstream [8].

6.4.2. Test Procedure

The procedure of the standard capillary threshold pressure is as follow:

- Open upstream valve (V1) and close downstream valve (V2).
- By using pump, increase the upstream pressure by one step (0.1 MPa) at a constant rate of 1 kPa/s.
- Monitor the pressure changes at the downstream for the estimated pressure diffusion time of approximately 23 minutes.
- For accuracy, it is recommended to observe the downstream pressure slightly more than the estimated pressure diffusion time. Therefore, we selected approximately 60 minutes for pressure diffusion time
- If there is no increase in the downstream pressure, again increase the upstream pressure by one step with the same flow rate, and observe the pressure changes at the downstream for the same time.
- Repeat the procedure until there is an increase in the downstream pressure.
- When the downstream pressure start increasing, this indicates that the capillary threshold pressure is achieved. Now the capillary threshold pressure can be calculated by simply taking the difference of upstream and downstream pressures ($P_c = P_{upstream} - P_{downstrem}$).

.

Chapter 07
Results and Discussion

7.1. Results

A series of two tests were performed by using standard approach to measure the capillary threshold pressure in Pierre and Field shale. Each test comprise of two phases, consolidation and the capillary threshold pressure phase. The experiments were conducted according to the procedure which was described in previous chapter.

7.1.1. Test 01

7.1.1.1. Consolidation Phase

In the first phase, after setting the sample, the confining pressure was increased at a constant rate of 0.9 MPa/hr. The maximum confining rate was calculated before the start of the test, and the confining rate used was adequately lower than the maximum confining rate. This has to done to protect the sample from any expected damages due to high confining pressure. The confining pressure was raised and set to a value of 20 MPa. This same value of confining pressure was used during the rest of the capillary threshold pressure phase. Table 7 shows the values of conning rate adopted during the tests.

The upstream and downstream pressure was also increased at a constant rate along with the confining pressure and set to a value of 10 MPa. During consolidation process, the confining pressure should be about 0.1 MPa higher than the both upstream and downstream pressure. The completion of consolidation phase was verified from deformation curves as shown in Figure 17.

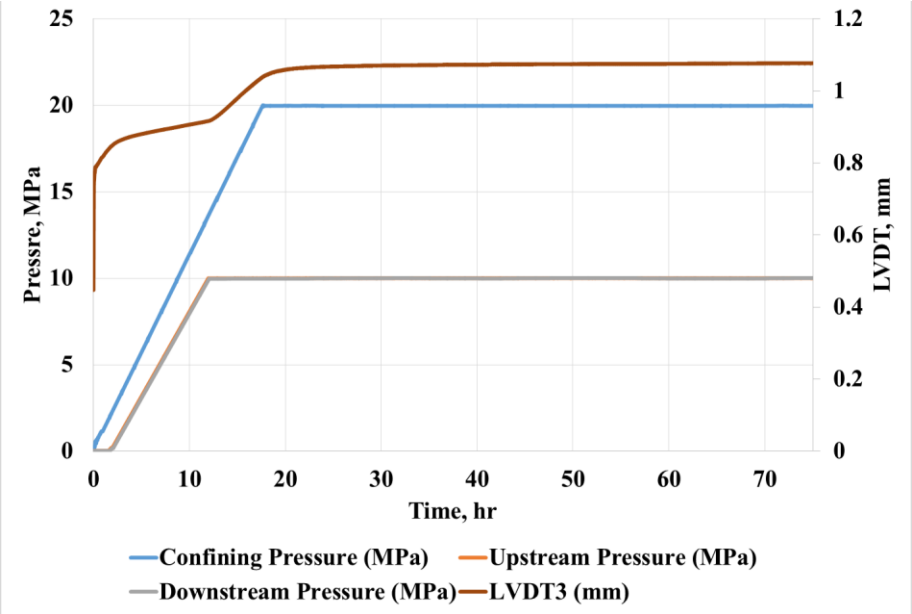

Figure 17: Consolidation phase of test 01

7.1.1.2. Capillary Threshold Pressure Test

The capillary threshold pressure measurement starts at a constant upstream and downstream presser of 10 MPa. While doing the first increment in the upstream pressure, due to a mistake there was a sudden drop in the upstream pressure from 10 MPa to 7.5 MPa. This fluctuation in pressure remains for a certain period of time and soon become stable.

The upstream pressure was than increase step-by-step, each step was of 0.1 MPa. The downstream pressure was monitored for pressure response for approximately 1 hour after every increase in upstream pressure. The downstream pressure starts increasing, when upstream pressure increase from 10.40 MPa to 10.50 MPa, as shown in Figure 18 and 19.

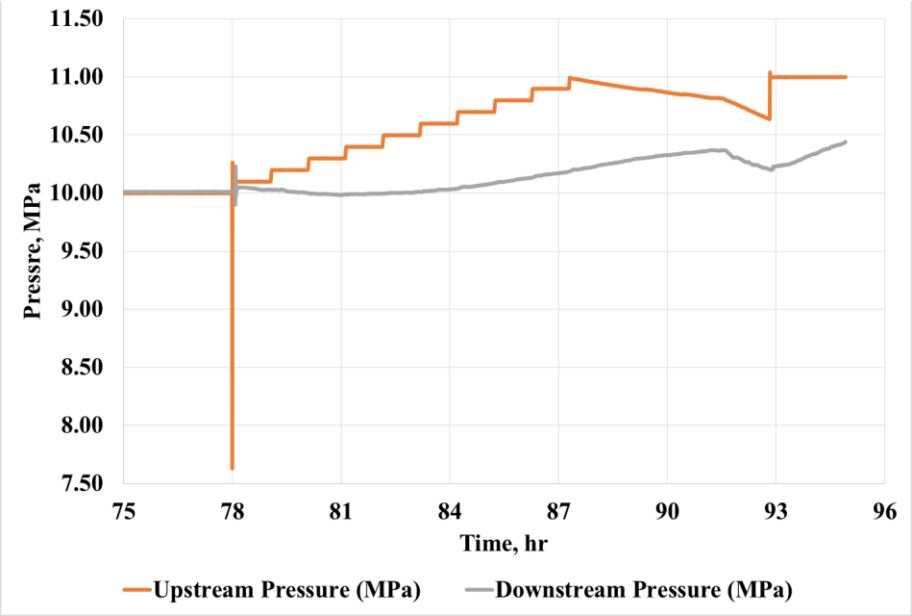

Figure 18: Pressure curves of capillary threshold pressure test 01

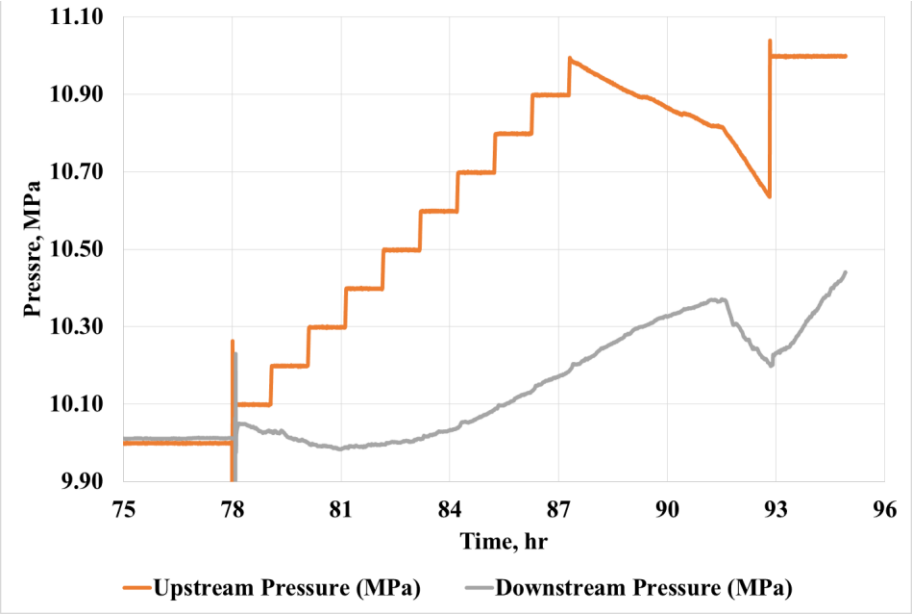

Figure 19: Pressure curves of capillary threshold pressure test 01 (zoom in)

7.1.2. Test 02

7.1.2.1. Consolidation Phase

The second test was conducted with maximum confining pressure of 10 MPa and maximum upstream and downstream pressure of 5 MPa. The selection of these values was based on the results of first test.

The maximum confining rate, calculated before the start of the test, was 0.3 MPa/hr. Therefore, the test was conducted with confining rate of 0.28 MPa/hr. The end of consolidation process was verified from the deformation curve. Figure 20 shows pressure and deformation curves during the consolidation phase.

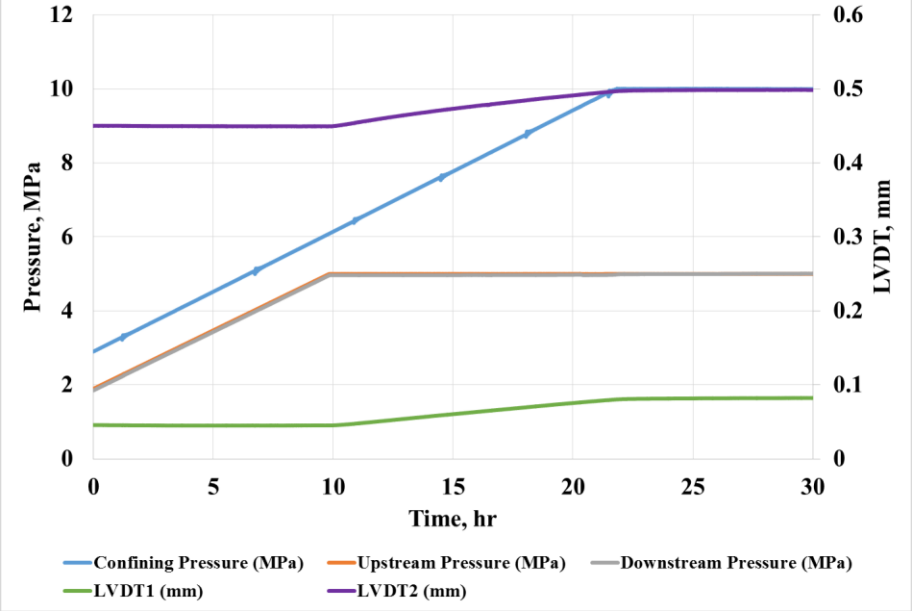

Figure 20: Consolidation phase of test 02

7.1.2.2. Capillary Threshold Pressure Test

The Figure 21 shows that, the capillary threshold pressure measured for test 2 was 0.3 MPa. The increase in upstream pressure shows a trend of a slight reduction in the downstream pressure. The downstream pressure first drop from 5 MPa to 4.90 MPa, than it stabilize with increase in upstream pressure.

The upstream pressure was increased step wise with each step of 0.1 MPa. The downstream pressure starts increasing, when upstream pressure rise from 5.20 MPa to 5.30 MPa. The

monitoring time for pressure response in downstream pressure was also 1 hour in this test. The capillary breakthrough pressure was also appears to be achieved, as there was a rapid increase in downstream pressure at the end. The capillary breakthrough pressure was 0.5 MPa.

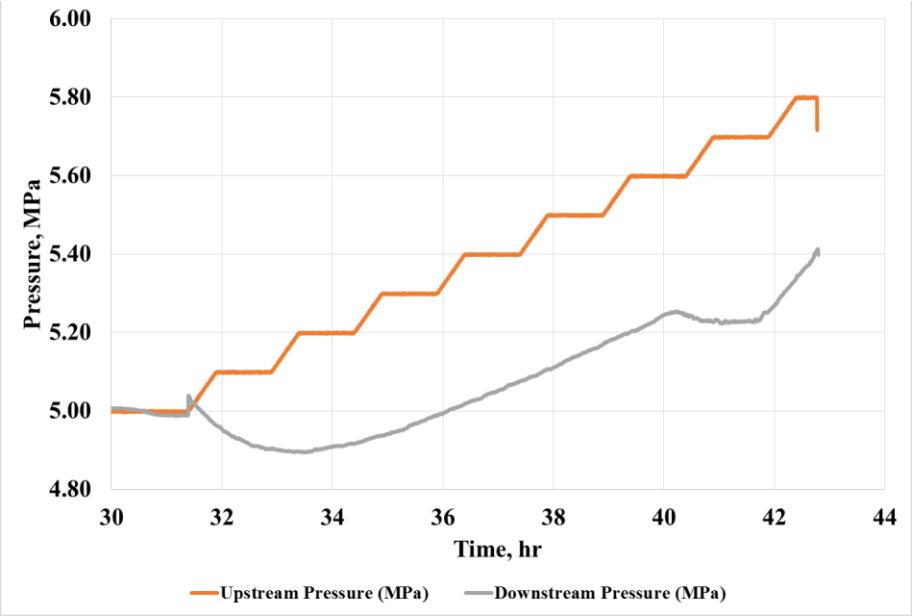

Figure 21: Pressure curves of capillary threshold pressure test 2

Table 7: Properties of shale for each test

Properties	Test 01	Test 2
Thickness (mm)	8.9	9.55
Radius (mm)	37.63	37.71
Weigh (gm)	23.24	24.12
C_d (m^2/s)	5.5E-08	5.5E-08
Δt (min)	22.8	22.8
Maximum confining rate (MPa/hr)	1.3	0.3
Confining rate used	0.9	0.28

7.2. Discussion

The shale samples used for the threshold capillary pressure test were at in-situ saturation conditions and neither dehydrated nor saturated with simulated pore fluid. This was done because the contact of sample with any fluid including simulated pore fluid can alter the properties of the sample, as the sample come in contact with bulk amount of water molecules and ions during saturation. This is in contrast with the downhole conditions where the sample is surrounded by the more shale.

The shale sample used for the first test was Pierre shale, saturated with 3.5% w/w NaCl brine and the non-wetting fluid was base oil. Since this was the first test, therefore more time was given for the consolidation process to make sure that all excessive pore pressure should be dissipated. However, Figure 17 shows that the deformation curve becomes straight after 20 hours and there was no further deformation of the sample. This indicates that the sample is completely consolidated. In the capillary threshold pressure part, while the first increment in upstream pressure from 10 MPa to 10.10 MPa, there was a sudden increase in upstream and downstream pressure from 10 MPa to 10.20 MPa and then a rapid decrease in upstream pressure to 7.50 MPa. This has been done by mistake and soon the situation was under control. Since the upstream pressure was decreased, therefore there was no serious negative effect on the final result. After the system become stable, the pressure was further increase and the capillary threshold pressure was achieved when the upstream pressure was increased from 10.40 MPa to 10.50 MPa. The capillary threshold pressure measured was 0.5 MPa.

From the experience of first test, the second test was performed and it takes less time for completion than the first test. In the second test the capillary threshold pressure was achieved when the upstream pressure was increased from 5.20 MPa to 5.30 MPa, and the capillary threshold pressure was 0.3. The Figure 21 shows that, at downstream pressure value of 5.20, there was an abrupt increase in the downstream pressure, which was also confirmed from the differential pressure data. This sudden increase in the downstream pressure indicates that wetting phase has been completely wiped off from the larger pores by non-wetting phase and the capillary breakthrough is achieved, and the capillary breakthrough pressure was 0.5 MPa.

Conclusion

The capillary threshold pressure measurement in shale was performed in the laboratory. The important finding and results are summarized below;

- The capillary threshold pressure measured for Pierre shale was 0.5 and for field shale was 0.3 MPa.
- The capillary breakthrough pressure for field shale was 0.5 MPa.
- Base oil was used as non-wetting phase for pressure measurement.
- Samples with in-situ saturation was used for the tests.
- The standard approach (step-by-step approach) was used to measure the capillary threshold pressure through shale.
- The standard approach is a time consuming but accurate method for capillary threshold pressure measurement.
- The efficiency of standard approach is largely base on the appropriate selection of pressure increment and time lapse for pressure diffusion.
- Necessary precautions should be taken during coring to avoid any interaction with other aqueous fluids.
- Temperature of the system should be kept constant during experiment, variation in temperature can affect the results.

Recommendations

- The equipment used for capillary threshold pressure can be utilized for the measurement of osmotic and swelling pressure in shale by doing some modifications in the equipment. The osmotic and swelling pressure measurement require continuous circulation, therefore both inlet and outlet valves are required for upstream piston.

- More capillary threshold pressure measurements must performed using oil-base mud as non-wetting phase.

- The other approaches for threshold capillary pressure measurement must also applied to correlate and verify the results obtained from the standard approach.

- The equipment must have temperature control system, so that the capillary threshold pressure measurements can be done at downhole temperature conditions.

Bibliography

1. van Oort, E., et al., *Transport in shales and the design of improved water-based shale drilling fluids.* SPE drilling & completion, 1996. 11(03): p. 137-146. SPE-28309-PA.

2. van Oort, E., *On the physical and chemical stability of shales.* Journal of Petroleum Science and Engineering, 2003. 38(3): p. 213-235.

3. Muniz, E.S., S.A. Fontoura, and R.F.T. Lomba. *Rock-drilling fluid interaction studies on the diffusion cell*. in *SPE Latin American and Caribbean Petroleum Engineering Conference*. 2005. Society of Petroleum Engineers.

4. Ewy, R.T. and R. Stankovic, *Shale swelling, osmosis, and acoustic changes measured under simulated downhole conditions.* SPE Drilling & Completion, 2010. 25(02): p. 177-186, SPE 78160 PA.

5. Chenevert, M.E. and V. Pernot, *Control of shale swelling pressures using inhibitive water-base muds.* SPE Annual Technical Conference and Exhibition, 1998.

6. Al-Bazali, T.M., et al. *An Experimental Investigation on the Impact of Capillary Pressure, Diffusion Osmosis, and Chemical Osmosis on the Stability and Reservoir Hydrocarbon Capacity of Shales*. in *Offshore Europe*. 2009. Society of Petroleum Engineers. SPE 121451.

7. Lal, M. *Shale stability: drilling fluid interaction and shale strength*. in *SPE Asia Pacific Oil and Gas Conference and Exhibition*. 1999. Society of Petroleum Engineers. SPE 54356.

8. Al-Bazali, T.M., *Experimental study of the membrane behavior of shale during interaction with water-based and oil-based muds.* PhD Dissertation, The University of Texas at Austin, 2005.

9. Mody, F.K. and A. Hale, *Borehole-stability model to couple the mechanics and chemistry of drilling-fluid/shale interactions.* Journal of Petroleum Technology, 1993. 45(11): p. 1,093-1,101. SPE 25728 PA.

10. van Oort, E. *Physico-chemical stabilization of shales*. in *International Symposium on Oilfield Chemistry*. 1997. Society of Petroleum Engineers. SPE 37263.

11. Ewy, R. and R. Stankovich. *Pore pressure change due to shale-fluid interactions: Measurements under simulated wellbore conditions*. in *4th North American Rock Mechanics Symposium*. 2000. American Rock Mechanics Association.

12. Skalle, P., *Drilling fluid engineering*. 2010: Bookboon.

13. Fjar, E., et al., *Petroleum related rock mechanics*. Vol. 53. 2008: Elsevier.

14. Pettersen Skippervik, C., *Study on the Swelling Potential of some Selected Rocks.* Master Thesis, Norwegian University of Science and Technology (NTNU), 2014.

15. Abass, H., et al. *Wellbore instability of shale formation; Zuluf field, Saudi Arabia*. in *SPE Technical Symposium of Saudi Arabia Section*. 2006. Society of Petroleum Engineers.

16. Fakcharoenphol, P., et al., *The effect of osmotic pressure on improve oil recovery from fractured shale formations.* SPE Unconventional Resources Conference, 2014.

17. Yew, C.H., C.L. Wang, and M.E. Chenevert. *A theory on water activity between drill-fluid and shale*. in *The 33th US Symposium on Rock Mechanics (USRMS)*. 1992. American Rock Mechanics Association.

18. Van Oort, E., A. Hale, and F. Mody. *Manipulation of coupled osmotic flows for stabilisation of shales exposed to water-based drilling fluids*. in *SPE Annual Technical Conference and Exhibition*. 1995. Society of Petroleum Engineers.

19. Ewy, R. and R. Stankovich. *Shale-Fluid Interactions Measured under Simulated Downhole Conditions, paper SPE*. in *ISRM 78160 presented at the SPE/ISRM Rock Mechanics Conference, Irving, Texas, 20-23 October 2002.* 2002. SPE 49263.

20. Al-Bazali, T.M., et al. *A Rapid, Rigsite Deployable, Electrochemical Test for Evaluating the Membrane Potential of Shales*. in *SPE Annual Technical Conference and Exhibition*. 2005. Society of Petroleum Engineers.

21. Muniz, E., S. da Fontoura, and R. Lomba. *Development of Equipment and Testing Methodology to Evaluate Rock-Drilling Fluid Interaction*. in *Gulf Rocks 2004, the 6th North America Rock Mechanics Symposium (NARMS)*. 2004. American Rock Mechanics Association.

22. Al-Bazali, T.M., et al. *Estimating the Reservoir Hydrocarbon Capacity Through Measurement of the Minimum Capillary Entry Pressure of Shale Caprocks*. in *SPE Annual Technical Conference and Exhibition*. 2009. Society of Petroleum Engineers.

23. Tiab, D. and E.C. Donaldson, *Petrophysics: theory and practice of measuring reservoir rock and fluid transport properties*. 2011: Gulf professional publishing.

24. Hildenbrand, A., S. Schlömer, and B. Krooss, *Gas breakthrough experiments on fine-grained sedimentary rocks.* Geofluids, 2002. 2(1): p. 3-23.

25. Egermann, P., J. Lombard, and P. Bretonnier, *A fast and accurate method to measure threshold capillary pressure of caprocks under representative conditions.* SCA2006 A, 2006. 46.

26. Smith, J.D., I. Chatzis, and M.A. Ioannidis, *A new technique for measuring the breakthrough capillary pressure.* Society of Core Analysis, SCA, 2002. 40: p. 2002.

27. Ito, D., et al., *Measurement of threshold capillary pressure for seal rocks using the step-by-step approach and the residual pressure approach.* Energy Procedia, 2011. 4: p. 5211-5218.

28. Kawaura, K., et al., *Examination of Methods to Measure Capillary Threshold Pressures of Pelitic Rock Samples.* Energy Procedia, 2013. 37: p. 5411-5418.

29. Augdal, C., *Measurements of the Capillary Entry Pressure in Shale.* Master Thesis, Norwegian University of Science and Technolohy (NTNU), 2014.

30. Al-Bazali, T.M., et al. *Factors controlling the membrane efficiency of shales when interacting with water-based and oil-based muds*. in *International Oil & Gas Conference and Exhibition in China*. 2006. Society of Petroleum Engineers.

31. Al-Bazali, T.M., et al. *Measurement of the sealing capacity of shale caprocks*. in *SPE Annual Technical Conference and Exhibition*. 2005. Society of Petroleum Engineers.

32. Zhang, J., et al. *A new gravimetric-swelling test for evaluating water and ion uptake in shales*. in *SPE Annual Technical Conference and Exhibition*. 2004. Society of Petroleum Engineers.

33. van Oort, E. *A novel technique for the investigation of drilling fluid induced borehole instability in shales*. in *Rock Mechanics in Petroleum Engineering*. 1994. Society of Petroleum Engineers.

34. Gao, S., et al., *Cap Rock CO 2 Breakthrough Pressure Measurement Apparatus and Application in Shenhua CCS Project.* Energy Procedia, 2014. 63: p. 4766-4772.

35. Simpson, J. and H. Dearing. *Diffusion Osmosis-An unrecognized cause of shale instability*. in *IADC/SPE Drilling Conference*. 2000. Society of Petroleum Engineers.

36. Osuji, C.E., M.E. Chenevert, and M.M. Sharma, *Effect of porosity and permeability on the membrane efficiency of shales.* SPE Annual Technical Conference and Exhibition, 2008.

37. Oleas, A., et al. *Entrance pressure of oil based mud into shale: effect of shale water activity and mud properties*. in *SPE Annual Technical Conference and Exhibition*. 2008. Society of Petroleum Engineers.

38. Klimkowski, Ł. and R. Smulski, *Laboratory Method to Measure Sealing Capacity of Caprocks/Metodyka Wykonywania Pomiarów Laboratoryjnych do Określania Własności Uszczelniających Skał Nadległych.* Archives of Mining Sciences, 2012. 57(2): p. 471-481.

39. Schlemmer, R., et al. *Membrane efficiency in shale-an empirical evaluation of drilling fluid chemistries and implications for fluid design*. in *IADC/SPE Drilling Conference*. 2002. Society of Petroleum Engineers.

40. Tan, C.P., et al. *Novel high membrane efficiency water-based drilling fluids for alleviating problems in troublesome shale formations*. in *IADC/SPE Asia Pacific Drilling Technology*. 2002. Society of Petroleum Engineers.

41. Carlos, J., D.E. Clark, and J. Zhang. *Stressed shale drilling strategy-water activity design improves drilling performance*. in *SPE Annual Technical Conference and Exhibition*. 2006. Society of Petroleum Engineers.

Appendix

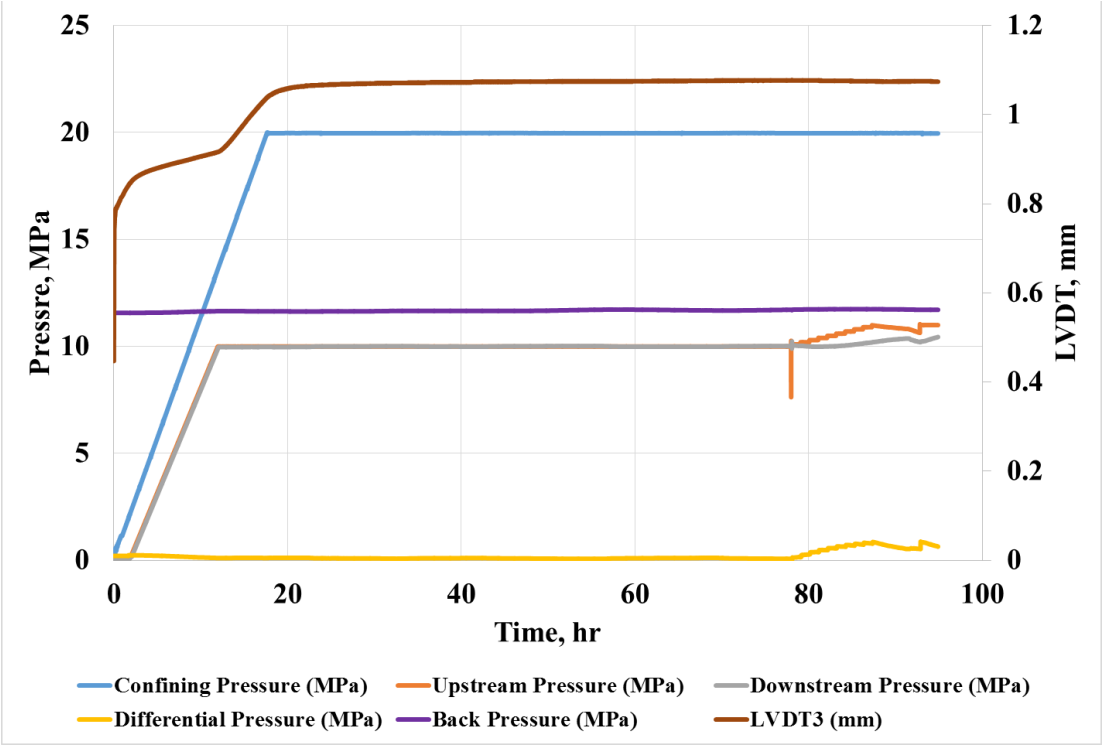

Figure A1: Capillary threshold pressure test 1

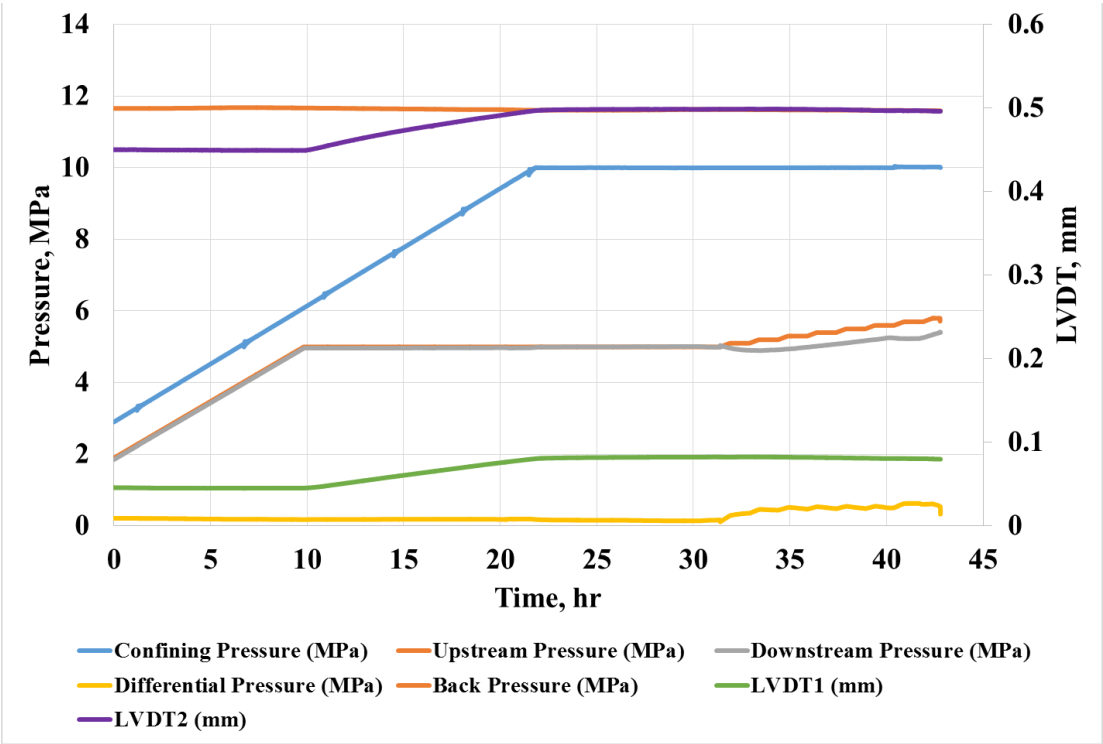

Figure A2: Capillary threshold pressure test 2

Table A1: Data set for capillary threshold pressure test 01

Test Type	
Sample ID	ML192_2_43
sample Name	Pierre shale
Project Number	
Operator	
Thickness	8.9
Radius	37.63
Weight	23.24
K_f [Pa]	2000000000
η_f [Pas]	0.001
φ	0.225
K_{fr} [Pa]	6630000000
G_{fr} [Pa]	535000000
k [D]	0.000000014
k [m^2]	1.38166E-20
1 D =	9.869E-13
C_d [m^2/s]	5.55602E-08
Pressure diffusion time	
l^2 [m^2]	7.62129E-05
Δt [s]	1371.717131
Δt [hrs]	0.381032536
Δt [min]	22.86195218
Rate of increasing confining pressure	
ΔP_{max} [MPa]	0.5
r [MPa/s]	0.000364507
r [MPa/hr]	1.31222
Expected Capillary threshold pressure	
σ [N/m]	0.03
θ [degrees]	20
θ [radians]	0.34906585
Pore throat rad. [m]	1.23E-08